Expression of Light Meromyosin in *Dictyostelium* Blocks Normal Myosin II Function

C. Geoffrey Burns,* Mary Reedy,* John Heuser,‡ and Arturo De Lozanne*

*Department of Cell Biology, Duke University Medical Center, Durham, North Carolina 27710; and ‡Department of Cell Biology, Washington University, St. Louis, Missouri 63110

Abstract. The ability of myosin II to form filaments is essential for its function *in vivo*. This property of self association is localized in the light meromyosin (LMM) region of the myosin II molecules. To explore this property in more detail within the context of living cells, we expressed the LMM portion of the *Dictyostelium* myosin II heavy chain gene in wild-type *Dictyostelium* cells. We found that the LMM protein was expressed at high levels and that it folded properly into α-helical coiled–coiled molecules. The expressed LMM formed large cytoplasmic inclusions composed of entangled short filaments surrounded by networks of long tubular structures. Importantly, these abnormal structures sequestered the cell's native myosin II, completely removing it from its normal cytoplasmic distribution. As a result the cells expressing LMM displayed a myosin–null phenotype: they failed to undergo cytokinesis and became multinucleate, failed to form caps after treatment with Con A, and failed to complete their normal developmental cycle. Thus, expression of the LMM fragment in *Dictyostelium* completely abrogates myosin II function in vivo. The dominant–negative character of this phenotype holds promise as a general method to disrupt myosin II function in many cell types without the necessity of gene targeting.

THE distribution of myosin II in nonmuscle cells is constantly changing according to the needs of the cells. During cytokinesis, for example, most myosin II assembles into filaments that localize to the contractile ring during anaphase and disassemble shortly thereafter upon completion of cell division. In a moving cell, myosin II resides in the trailing edge; however myosin must change its localization rapidly when a cell changes direction and forms a new trailing edge. One possible mechanism for such dramatic reorganization of myosin II molecules is via a precise regulation of myosin filament assembly in a spatial and temporal manner. A second possible means to change myosin II distribution would be to move the myosin II filaments along actin filaments to particular cellular locations. However, we currently know little about the relative contribution of filament assembly vs. filament movement to the spatial organization of myosin II in living cells.

The tail portion of *Dictyostelium* myosin II contains two domains involved in filament formation and its regulation. The carboxyl-terminal 34-kD segment of the myosin tail (C-light meromyosin [LMM]-34)[1] contains three phosphorylation sites which regulate filament formation in response to a chemotactic signal (Berlot et al., 1987; Vaillancourt et al., 1988; O'Halloran et al., 1990). This domain is adjacent to an internal 34-kD domain (N-LMM-34) that is necessary and sufficient for filament formation (O'Halloran et al., 1990). These two domains constitute the LMM portion of the *Dictyostelium* myosin II molecule (De Lozanne et al., 1987).

Several *Dictyostelium* myosin II mutants have been constructed with different deletions within the myosin tail region. Deletion of the S2 portion between the LMM and the myosin heads produces a fully functional myosin molecule (Kubalek et al., 1992). Deletion of the regulatory C-LMM-34 domain produces myosin II molecules that form filaments but are not properly regulated; surprisingly, even though these mutant molecules form large aggregates in the cell they still perform most known myosin functions (O'Halloran and Spudich, 1990; Egelhoff et al., 1991). Deletion of the entire LMM portion produces a myosin II molecule that is unable to form filaments and, as a result, is not functional in vivo (De Lozanne and Spudich, 1987; Fukui et al., 1990). These deletion mutants highlight the importance of the LMM portion of the myosin molecule for proper myosin II function and distribution within living cells.

To explore in better detail the contribution of the LMM domain to the distribution of myosin II in vivo, we expressed this domain in *Dictyostelium* wild-type cells. We expected this domain to coassemble with wild-type myosin

Address all correspondence to A. De Lozanne, Department of Cell Biology, Box 3709, 367 Nanaline Duke Building, Duke University Medical Center, Durham, NC 27710. Tel.: (919) 681-6851. Fax: (919) 681-7978.

1. *Abbreviations used in this paper*: aa, amino acid; LMM, light meromyosin; MHC, myosin II heavy chain.

II into filaments and to localize correctly. Surprisingly, we found that expression of the LMM fragment led to the complete loss of myosin II function, and thereby caused a dominant-negative phenotype.

Materials and Methods

Design of Expression Vectors

The expression vector used in this paper was based on plasmid pBS18 (kindly provided by Dr. Richard Firtel, University of California, San Diego, CA.). This vector contains a G418 selectable marker under the control of the actin 6 promoter and the actin 15 terminator. We modified this vector to express epitope-tagged proteins under the control of the actin 15 promoter and the SP70 terminator. This vector, pAD80HA, encodes an initiation methionine followed by the sequence recognized by the monoclonal antibody 12CA5 (YPYDVPDYA). The epitope tag is followed by the restriction sites NcoI, KpnI, EcoRI, BglII, HindIII, and KpnI. These sites were incorporated for the cloning and expression of specific myosin II heavy chain (MHC) fragments.

To obtain an expression vector containing the LMM fragment we first cloned the entire myosin tail coding region (4.2-kb NcoI-SmaI fragment from pBgl4.5 [De Lozanne, 1988]) into the NcoI-EcoRI (blunted) sites of pAD80HA yielding plasmid pAD80HA-ROD. From this plasmid we isolated a 2.1-kb KpnI fragment encoding the LMM fragment and subcloned it into the KpnI sites of pAD80HA to yield plasmid pAD80HA-LMM. Therefore this vector expresses a fusion protein containing the epitope tag followed by the LMM fragment (from amino acid [aa] 1528 to aa 2116 of the MHC sequence). The predicted molecular weight for this fusion protein is 70 kD.

Cell Culture Growth, Transformation, and Test for Growth in Suspension

Dictyostelium discoideum axenic strain, AX2, was grown in HL5 media by standard methods (Spudich, 1987). Cells were transformed with plasmid pAD80HA-LMM by electroporation and clonal transformants were obtained in 2–3 wk by selection in 10 μg/ml G418. All cell lines were maintained on Petri dishes in HL5 medium containing G418. Individual cell lines were tested for their ability to grow in suspension by monitoring the titer of shaking cultures over a period of several days. As a control we used a transformed cell line with plasmid pAD80HA-ROD that did not express any myosin fragments and that displayed a phenotype indistinguishable from untransformed cells.

Analysis of LMM Expression

The expression of LMM in the transformed cells was analyzed by Western blots and Coomassie blue–stained polyacrylamide gels. Briefly, *Dictyostelium* transformed cells were harvested and lysed at a concentration of 1×10^8 cells/ml in 50 mM Tris (pH 8.0), 20 mM sodium pyrophosphate, 5 mM EDTA, 5 mM EGTA, 0.5% Triton-X 100, and a cocktail of protease inhibitors. Cell extracts from a total of 1×10^6 cells per lane were separated on a 7.5% SDS–polyacrylamide gel. Protein was transferred to nitrocellulose, and then probed with polyclonal antisera raised against the *Dictyostelium* LMM or S2 regions (see below). The blot was incubated with an HRP-conjugated goat anti–rabbit antibody and developed by color reaction with 4-chloro-napthol and hydrogen peroxide.

To quantitate the relative proportions of LMM and MHC, the cell lysate was serially diluted and processed for Western blot analysis as before. The same samples were separated on a 7.5% polyacrylamide gel, and the gel stained with Coomassie brilliant blue. The developed Western blot and the destained gel were scanned on a HP desk scanner using DeskscanII software and the relative protein amounts were quantified using NIH image 1.54.

Antibodies

We used two rabbit antisera raised specifically against the S2 or the LMM region of the *Dictyostelium* myosin tail (Shoffner, J. D., and A. De Lozanne, unpublished data). These regions were expressed in *Escherichia coli*, purified to homogeneity and injected into rabbits. Antibody 9555-3 was raised against a myosin fragment encompassing most of the LMM region and a portion of the S2 region (from aa 1401 to aa 2034 of the MHC sequence). This antibody recognizes MHC and LMM proteins (Fig. 2). Antibody 9558-2 was raised against a fragment from the myosin S2 region (from aa 883 to aa 1528 of the MHC sequence). This antibody binds to MHC but not to the LMM protein (Fig. 2).

A monoclonal antibody, 12CA5, recognizes the HA epitope YPYDVPDYA engineered in our *Dictyostelium* expression vector and was obtained from Berkeley Antibodies, Co. (Berkeley, CA). This antibody was preabsorbed against fixed and permeabilized *Dictyostelium* cells to remove background reactivity. Large batches of *Dictyostelium* cells were washed and fixed in 3.7% formaldehyde in Sorenson's buffer (14.6 mM KH_2PO_4 and 2 mM Na_2HPO_4, pH 6.1) for 5 min. The fixed cells were then permeabilized in 0.5% Triton X-100 in Sorenson's buffer for 5 min. The 12CA5 antibody was preabsorbed on these cells until it showed no immunofluorescence reactivity on wild-type *Dictyostelium* cells. The preabsorbed 12CA5 antibody recognizes specifically the epitope-tagged LMM protein (see Fig. 2).

Analysis of Triton Cytoskeletons

LMM mutants and control cells were harvested, washed, and lysed at a concentration of 2×10^7 cells/ml in cold lysis buffer (100 mM MES, pH 6.8, 1 mM $MgCl_2$, 0.5% Triton-X 100, 2.5 mM EGTA, and a cocktail of protease inhibitors) in the presence or absence of 100 mM ATP. Lysates were centrifuged for 30 s in a microcentrifuge to pellet the cytoskeletons. Supernatants were collected and the cytoskeletal pellets were resuspended in the same volume of lysis buffer. Fractionated extracts from 1×10^6 cells/lane were run on a 7.5% SDS–polyacrylamide gel, transferred to nitrocellulose, and probed with antiserum 9555-3 as described above.

Analysis of the Folding and Assembly Characteristics of the Expressed LMM

To determine if the LMM protein was folded into an α-helical coiled–coil we tested its sensitivity to heat denaturation. Cytoskeletal pellets of LMM mutant and control cells were prepared as described above in the absence of ATP. Such pellets were resuspended in 0.6 M NaCl, 20 mM Tris (pH 7.5), 5 mM EDTA, and 1 mM ATP. Samples were placed in a boiling water bath for 10 min, cooled, and centrifuged for 10 min in a microcentrifuge. Supernatants were collected and pellets resuspended the same volume of SDS-containing sample buffer. Equivalent amounts of both fractions were analyzed by SDS–polyacrylamide gel electrophoresis as described above.

To test if the LMM protein had assembly characteristics similar to those of myosin II, we determined the solubility properties of both proteins in buffers of high ionic strength. Cytoskeletal pellets such as those described above were resuspended in 0.6 M NaCl, 20 mM Tris (pH 7.5), 5 mM EDTA, 1 mM ATP and centrifuged at 100,000 *g* in a TL-100 rotor for 30 min. The supernatant and pellet fractions were analyzed as described above.

Light Microscopy

To determine the number of nuclei per cell we stained the cells with DAPI. LMM mutant and control cells were allowed to attach to coverslips, fixed for 5 min at –20°C in 1% formaldehyde in methanol, and incubated with 0.1 μg/ml DAPI for 15 min at room temperature. Stained cells were washed, mounted, and viewed under UV light.

To determine the localization of myosin and LMM in the cells we immunostained them with the antibodies described above. LMM mutant and control cells were allowed to attach to coverslips, and fixed for five minutes at −20°C in 1% formaldehyde in methanol. Fixed cells were washed and incubated for 30 min at 37°C with antibody dilution buffer (50 mM Tris, pH 7.5, 150 mM NaCl, 5% BSA, 0.02% NaN_3). Cells were incubated with a 1:1,000 dilution of antiserum 9558-2 or a 1:50 dilution of 12CA5 antibody in antibody dilution buffer and incubated at 37°C for 1 h. Samples were washed in 50 mM Tris (pH 7.5), 150 mM NaCl, and incubated with preabsorbed FITC-conjugated goat anti–rabbit or goat anti–mouse antibodies (30 μg/ml in antibody dilution buffer) at 37°C for 1 h. Samples were washed, mounted, and viewed by epifluorescence microscopy.

To determine the localization of actin, the LMM mutant and control cells were allowed to attach to coverslips. Cells were fixed for ten minutes at room temperature in 3.7% formaldehyde in Sorenson's buffer containing 150 mM KCl, 5 mM $MgCl_2$, and 10 mM EGTA. Fixed cells were washed and incubated with 0.7 U/ml rhodamine-conjugated phalloidin

(Molecular Probes, Eugene, OR) in 137 mM NaCl, 2.7 mM KCl, 10.1 mM Na_2HPO_4, 1.8 mM KH_2PO_4 (pH 7.2), 0.05% Triton X-100 . Stained cells were rinsed, mounted, and viewed by epifluorescence microscopy.

Capping of Con-A Receptors

LMM mutant and control cells were allowed to attach to coverslips. Cells were washed and incubated for one minute in 0.5 mg/ml FITC-conjugated ConA (Sigma Chemical Co., St. Louis, MO) in Sorenson's buffer. The ConA solution was removed and replaced with Sorenson's buffer. At 5, 10, 15, and 30 min time points thereafter, samples of both cell types were fixed for 5 min at –20°C in 1% formaldehyde in methanol. Fixed cells were washed, mounted, and viewed by epifluorescence microscopy.

Video Microscopy

Dictyostelium amoebae were mounted in phosphate buffer in a Zigmond chamber on a standard light microscope and viewed with a 63× 1.4 NA phase–contrast objective. They were viewed at extremely low light levels by video enhancement with a Hamamatsu CT2400 SIT camera coupled to an Argus 10 video processor set for eight-frame averaging. Time-lapse records were obtained by storing one video image per second in a Panasonic TQ 3038 laser disk recorder. Optimal sequences were printed on 4 1/2-in thermal paper with a Sony UP-860 video graphic printer, and then photographically reduced to produce montages.

Thin Section Electron Microscopy

LMM mutant and control cells were allowed to attach to thermanox coverslips for 2 h. Cells were rinsed and fixed for 30 min at room temperature in 3% glutaraldehyde, 0.2% tannic acid (Mallinckrodt), 20 mM potassium MOPS (pH 6.8), 5 mM EGTA, 5 mM NaN_3, and 5 mM $MgCl_2$. Cells were rinsed and post-fixed for 20 min on ice in 1% OsO_4, 0.1 M potassium phosphate (pH 6.0), and 10 mM $MgCl_2$. Cells were rinsed and stained for 30 min on ice in 2% uranyl acetate in water. Cells were rinsed and dehydrated stepwise from 50 to 100% ethanol. Dehydrated cells were embedded with Araldite 506 Reedy Mix for 48 h at 65°C. Gray sections were cut on a Reichert OMU3 ultramicrotome, picked up on carbon coated grids, and stained with 2% $KMnO_4$ / Sato lead (Reedy and Reedy, 1985). Photographs were taken on a Philips EM300 on SO163 film.

Freeze-etch Electron Microscopy

Dictyostelium amoebae were quick-frozen by abrupt application of a pure copper block cooled to LN_2 temperature, then freeze–fractured and deep etched in a Balzers device according to standard procedures (Heuser, 1989). Platinum replicas of the freeze-etched *Dictyostelium* were then prepared and examined in a standard transmission electron microscope operated at 100 kV. Images were photographically reversed to make platinum deposits appear white.

Analysis of Dictyostelium Development

The ability of the LMM mutant and control cells to complete the *Dictyostelium* developmental program was assayed according to standard procedures. Lawns of *Klebsiella aerogenes* were grown on SM/5 nutrient agar plates and were then inoculated with LMM mutant and control cells. Inoculated plates were observed for several days to assess the degree of clearing of the bacterial lawn and then the progress through the *Dictyostelium* developmental cycle.

Results

Expression of LMM

To test the ability of LMM to colocalize with myosin II in vivo, we expressed LMM in *Dictyostelium* wild-type cells. We designed a *Dictyostelium* expression vector containing an epitope tag (recognized by monoclonal antibody 12CA5) at the amino terminus of LMM (Fig. 1). This vector was introduced into *Dictyostelium* wild-type (Ax2) cells and clonal transformed cell lines were isolated. Western blot analysis of total cell lysates from transformed cells showed that

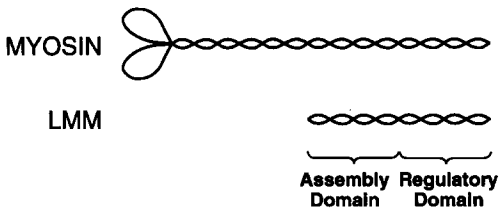

Figure 1. Expression of light meromyosin (LMM) in *Dictyostelium.* LMM is the region of the myosin II molecule that contains the domains required for filament formation and regulation. This region of the myosin II heavy chain gene (from aa 1528 to aa 2116) was cloned into an expression vector designed to incorporate an epitope tag at the amino terminus of the expressed LMM (see Materials and Methods).

they expressed large amounts of LMM (Fig. 2). As expected, the expressed LMM fragment was specifically recognized by the 12CA5 antibody (Fig. 2). Densitometric analysis of such blots revealed that the LMM fragment was expressed at a 10:1 molar ratio with respect to the endogenous myosin heavy chain (MHC). We attempted to obtain cell lines that expressed LMM at a lower level, however, analysis of many independent transformants indicated that all expressed the same high levels of LMM. In contrast, the levels of expression of other myosin tail fragments (S2 and Rod fragments) using the same vector reached only a 1:1 molar ratio with respect to the endogenous MHC (Burns et al., 1995).

Biochemical Properties of LMM

Initially, we wanted to determine if the expressed LMM associated with the actin cytoskeleton in a manner similar to myosin II. To do this, we analyzed the composition of Triton X-100 cytoskeletal extracts made from transformed and control cells in different buffer conditions. As expected, myosin II from control cells sedimented with the actin cytoskeleton in the absence but not in the presence of ATP (Fig. 3 *A*). In contrast, both myosin II and LMM from the transformed cells sedimented with the actin cytoskeleton under all conditions (Fig. 3 *A*). This result suggested that the presence of LMM disrupted the normal ATP-sensitive association of myosin II with the actin cytoskeleton. This was confirmed by the structural work pre-

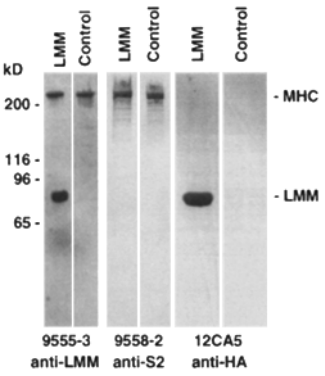

Figure 2. LMM is highly expressed in *Dictyostelium* transformed cells. Western blot analysis of the LMM and control cells shows that the LMM protein is expressed at high levels and that it is properly tagged. When the blot is stained with an anti-LMM antibody (9555-3) both myosin and LMM are detected. From dilution series of similar blots we found that LMM is expressed at a 10:1 molar ratio with respect to myosin heavy chain. An anti-S2 antibody (9558-2) recognizes only myosin and not LMM. The monoclonal antibody 12CA5 recognizes specifically the epitope tag at the amino terminus of LMM.

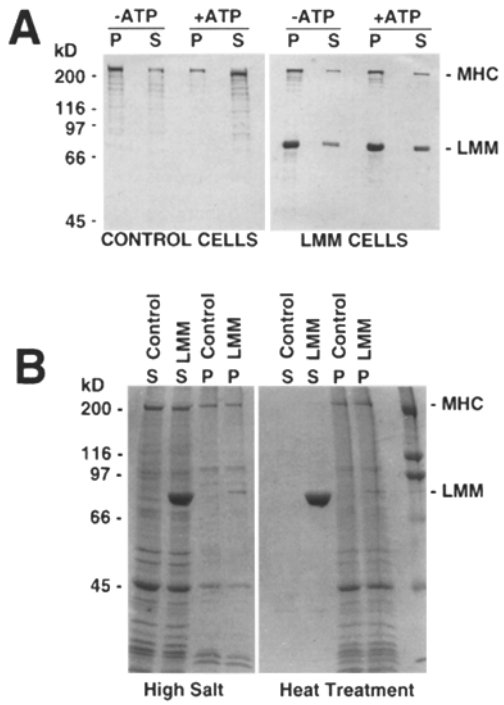

Figure 3. Biochemical properties of the expressed LMM. (*A*) Sedimentation of Triton X-100 cytoskeletons. LMM and control cells were lysed in a buffer containing Triton X-100 with or without ATP and centrifuged. The pellet and supernatant fractions were analyzed by Western blots using antibody 9555-3. In control cells myosin II sediments with the Triton X-100 cytoskeleton in the absence but not in the presence of ATP. In the LMM cells, both myosin and LMM sediment in both conditions. *P*, pellet fraction; *S*, supernatant fraction. (*B*) Solubility and heat resistance of LMM. Triton cytoskeletons were prepared from LMM and control cells in the absence of ATP as shown in *A*. The pellet fractions were then resuspended in a high ionic-strength buffer and either sedimented at 100,000 *g* for 30 min (*High Salt*) or placed in a boiling water bath for 10 min before centrifugation (*Heat Treatment*). The supernatant and pellet fractions were then analyzed by polyacrylamide-gel electrophoresis and the gels stained with Coomassie blue. Both myosin II and LMM are released into the supernatant fraction by the high salt treatment. On the other hand, only LMM remains in the supernatant fraction after heat treatment.

sented below, which demonstrates that in these cells myosin II associates with LMM in large aggregates. These presumably hold together and sediment with the cytoskeleton regardless of the presence or absence of ATP.

To determine if the expressed LMM folded properly into an α-helical coiled–coil we exploited the remarkable property of coiled–coiled proteins of resistance to heat denaturation. We subjected a Triton X-100 cytoskeletal extract from the LMM expressing cells to heat denaturation and subsequent centrifugation. We found LMM to be the only protein remaining in solution in the supernatant (Fig. 3 *B*). All other proteins (including myosin II) denatured and precipitated (Fig. 3 *B*). The solubility of the LMM protein after heat treatment suggests that it is correctly folded into a coiled–coil. Myosin II, which also has a coiled–coil tail, was found in the pellet fraction because its globular head was denatured by the heat treatment.

Further evidence that the expressed LMM protein folds properly is that it exhibits solubility properties typical of myosin II and its fragments. Both the expressed LMM and the endogenous myosin II were soluble in high ionic strength buffers and insoluble in low ionic strength buffers (Fig. 3 *B*). Taken together these experiments show that the expressed LMM forms a native coiled–coil capable of association into sedimentable filamentous structures. However, despite these native properties, LMM disrupts the normal interaction of myosin II with actin in the Triton X-100 cytoskeletons.

LMM Produces a Myosin Null Phenotype

To explore the physiological consequences of LMM overexpression, we examined the ability of the LMM cells to carry out cellular functions mediated by myosin II: cytokinesis, capping of Con A receptors and development (De Lozanne and Spudich, 1987; Fukui et al., 1990). To our surprise, the cells expressing LMM displayed a myosin null phenotype. These cells could not grow in suspension cultures (Fig. 4) because they failed to undergo cytokinesis. As a result, they became very large and multinucleate (Fig. 5 *B*) in a manner identical to the previously described myosin II null mutants (Manstein et al., 1989). Under the same conditions, the control cells grew at a normal rate (Fig. 4) and contained a single nucleus (Fig. 5 *A*).

To examine the ability of these cells to cap cell surface receptors, we challenged control and LMM cells with FITC-labeled Con A and incubated them for increasing amounts of time before fixation and observation. The LMM cells failed to cap their Con A surface receptors even after 30 min of treatment (Fig. 5 *D*). In contrast, the control cells readily formed caps within 5 min (Fig 5 *C*).

To test for phagocytosis and development, we plated control and LMM cells on a lawn of bacteria on an agar plate. The control cells cleared the bacterial lawn at the inoculation site within a day and the colony then expanded quickly beyond this site (data not shown). Once the control cells depleted the bacteria, they initiated the *Dictyo-*

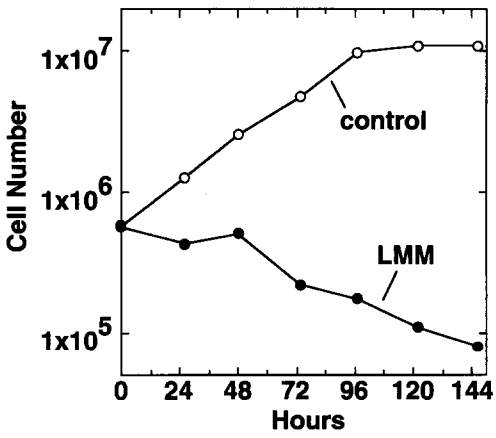

Figure 4. LMM cells cannot grow in suspension cultures. LMM and control cells were harvested from plate cultures and placed in suspension cultures at an initial titer of 1×10^5 cells/ml. The control cells grew until they reached saturation whereas the LMM cells failed to grow. This phenotype is identical to that of myosin II null mutants.

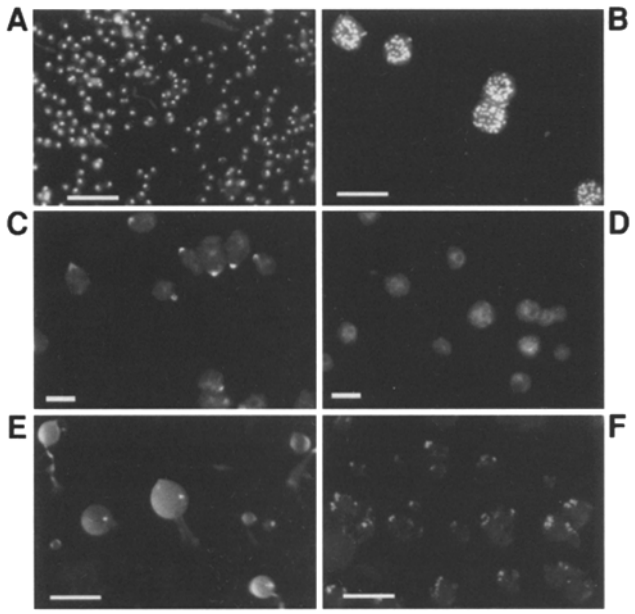

Figure 5. LMM cells have a myosin II null phenotype. (*A* and *B*) Cytokinesis. After two days in suspension cultures as in Fig. 4, LMM and control cells were fixed and stained with DAPI. In contrast to the control cells which are uninucleate (*A*), the LMM cells become large and multinucleate (*B*). (*C* and *D*) Capping. LMM and control cells were challenged with FITC-labeled Con A, fixed, and visualized by epifluorescence microscopy. Control cells cap their Con A receptors within 5 min (*C*) whereas the LMM cells do not form any caps even after 30 min (*D*). (*E* and *F*) Development. LMM and control cells were placed under starvation conditions to trigger the *Dictyostelium* developmental program. Both strains complete the initial stages of development but the LMM cells arrest at the mound stage (*F*). In contrast the control cells go on to make mature fruiting bodies (*E*). Bars: (*A* and *B*) 50 μm; (*C* and *D*) 10 μm; and (*E* and *F*) 1 mm.

stelium developmental program and formed mature fruiting bodies (Fig. 5 *E*). In contrast, the LMM cells were slower in clearing the inoculation site by a day or two, expanded slowly beyond this site and were unable to complete the developmental program beyond the mound stage (Fig. 5 *F*).

These results are identical to those obtained with myosin null cells (Manstein et al., 1989; Fukui et al., 1990). Therefore the LMM cells are a phenocopy of the myosin null cells.

LMM Sequesters Myosin into Filamentous and Tubular Structures

To understand why the expression of LMM in *Dictyostelium* cells produces a myosin null phenotype we examined the intracellular localization of LMM and myosin in these cells by immunofluorescence microscopy using antibodies specific for either protein. To detect the LMM molecules we used monoclonal antibody 12CA5 which binds specifically to the epitope tag on the LMM protein (Fig. 2). To detect the full-length myosin II molecules we used a polyclonal anti-myosin S2 antibody which does not bind to the LMM protein (Fig. 2). As expected in control cells, the 12CA5 antibody did not detect any structure (Fig. 6 *A*)

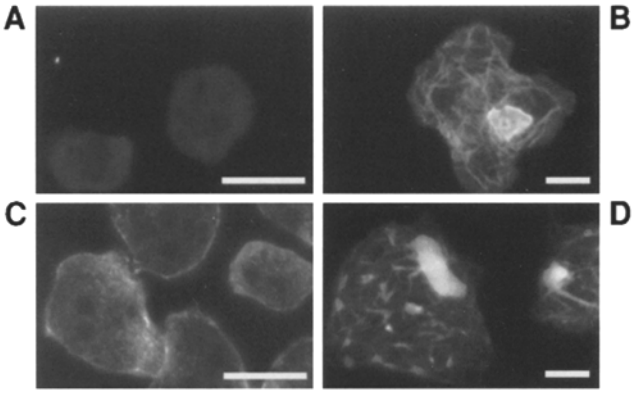

Figure 6. LMM sequesters myosin II into filamentous structures. LMM and control cells were fixed and stained with a monoclonal antibody (12CA5) specific for the epitope tag on the LMM protein (*A* and *B*) or with a polyclonal antibody (9558-2) specific for the myosin S2 region (*C* and *D*). Control cells only stain with the anti-S2 antibody and display the normal cortical distribution of myosin II (*A* and *C*). In contrast, both antibodies stain the same remarkable structures in the LMM cells (*B* and *D*). These cells contain a very large and round structure in their cytoplasm as well as a network of long and thin filamentous structures. By observing different focal planes of these cells we noticed that these later structures are closely associated with the cortex of the cell. Bar, 10 μm.

while the anti-S2 antibody revealed the typical myosin II distribution in the cortex of the cell (Fig. 6 *C*). In contrast, both antibodies labeled unique structures in the LMM cells (Fig. 6, *B* and *D*). We observed large globular structures in the cytoplasm of these cells as well as extended arrays of long, narrow structures. By observing these cells at different focal planes we found that these extended arrays were mostly associated with the cortex of the cell. The size and shape of these long structures suggested that they may represent LMM paracrystals. *Dictyostelium* LMM paracrystals prepared in vitro have been shown to be well ordered and able to diffract (O'Halloran et al., 1990). To determine if the mutant cells contained LMM paracrystals we observed them under a polarized light microscope since paracrystals should be strongly birefringent. To our surprise, we found only a few examples of birefringent structures in these cells, but not as many as the immunofluorescence microscopy suggested (data not shown).

To resolve the exact nature of the structures found in the LMM cells we analyzed them by thin-section microscopy. We found that these mutant cells contained remarkable structures never observed in wild-type cells. The expressed LMM induced the formation of short filamentous structures about 0.5-μm long and 0.1-μm thick which were occasionally found in isolation (Fig. 7 *A*) but were mostly found in large clusters near the cortex of the cell (Fig. 7 *B*). The short filaments in these clusters were oriented in all directions, were straight and did not branch. The size and shape of these filament clusters were consistent with those of the large structures observed by immunofluorescence microscopy. The random orientation of the filaments within the cluster also explained its lack of birefringence in polarized light microscopy.

In addition to the clusters we found very long structures

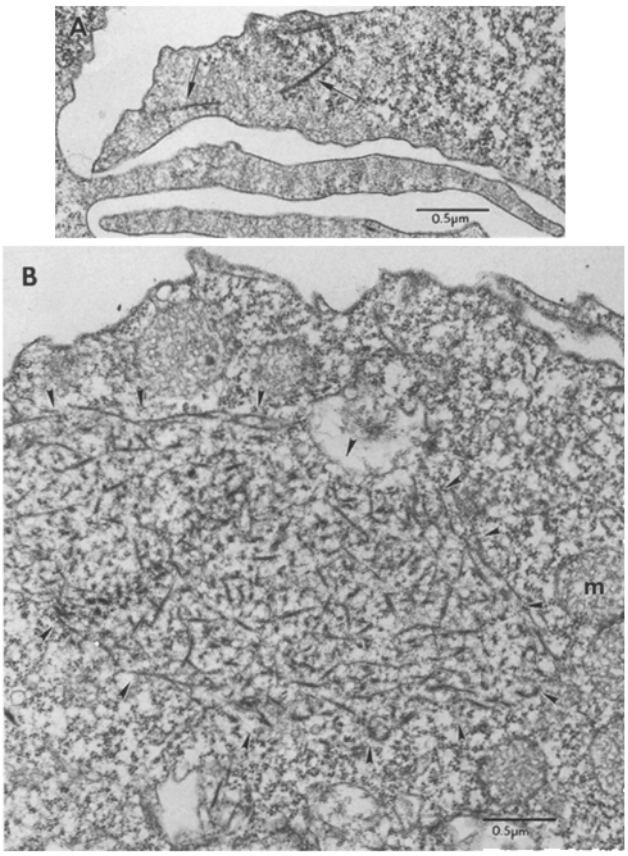

Figure 7. LMM cells contain discrete aggregates of short filaments and some individual filaments in the actin cortex. *A* shows two individual filaments (*arrows*) in the actin-rich cortical cytoskeleton. The large aggregates, like the one shown in panel *B*, are the most obvious characteristic of LMM cells. These aggregates (delimited by the *arrowheads*) contain short filaments distributed in all directions. These aggregates give rise to the large fluorescent structures seen by light microscopy. The aggregates exclude all organelles including mitochondria (*m*), ribosomes, and vesicles.

also associated with the cortex of the cell (Fig. 8). These structures were organized as long tubes which appeared to exclude organelles from their lumen (Fig. 8, *large arrows*). These tubular structures had a diameter of about 0.1–0.2 μm and could extend the entire length of the cell. These structures were usually not very straight and also showed branching. In addition, they were frequently found clustered in parallel arrays closely associated with the plasma membrane. These tubular structures correlated with the size and distribution of the long structures observed by immunofluorescence microscopy. We do not think that these structures represent tubular filaments because their diameter is much larger than that of the tubular myosin filaments found in insect flight muscles (Beinbrech et al., 1988).

These unique structures in LMM cells were readily visible also in platinum replicas of amoebae that were quick–frozen without prior chemical fixation. By freeze–fracturing and deep etching such amoebae, views of their cytoplasmic interiors were obtained that clearly displayed the large aggregates of LMM as well as the tubular structures (Fig. 9).

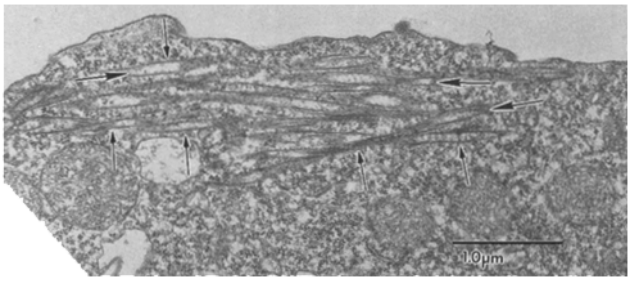

Figure 8. LMM cells contain tubular structures. The LMM cells contain long tubular structures which are often clustered in parallel arrays near the cortex of the cells. This micrograph shows one of these clusters. The lumen of these tubular structures (*large arrows*) is clearly distinct from the cytoplasm of the cell. The small arrows indicate the walls of these structures.

The large aggregates appeared as a dense and uniform meshwork that excluded all organelles (Fig. 9 *A*). The tubular structures appeared as loose bundles of ~15-nm-diam fibrils that ran roughly parallel to each other along the length of the tubes (Fig. 9 *B*).

The organization of the short filaments in the large clusters was intriguing. The aggregates displayed many fine fibrils interspersed among the thicker filaments (Fig. 7 *B*). These fibrils appeared to hold the filaments so tightly that, overall, the aggregates excluded all other cytoplasmic organelles, including even ribosomes as well as larger membranous organelles and mitochondria. We thought that this cluster might be held together by the interaction of actin filaments with myosin II heads found in the cluster. However, when we stained the LMM mutant cells with rhodamine-labeled phalloidin we found that actin filaments were not present within or around the large clusters (Fig. 10).

Due to the exclusion of organelles, the large clusters of short filaments were clearly visible by phase contrast or DIC microscopy. Time-lapse microscopy of the LMM cells revealed that the large clusters were not static structures but instead were dynamic and malleable. The clusters moved around passively within the cell during amoeboid movement. Often they fragmented into smaller clusters or even penetrated to the very edges of the actin-rich region of the pseudopods of the cell (data not shown).

Discussion

The ability to self associate into thick filaments is a property common to all known myosin II molecules. This property has been localized to defined regions within the LMM portion of the myosin II tail (Nyitray et al., 1983; O'Halloran et al., 1990; McNally et al., 1991; Lee et al., 1994). Although the importance of these regions for filament formation has been demonstrated, it is still not understood how they interact with each other to form filaments. To begin to investigate this problem we developed a system for the expression of LMM in *Dictyostelium* cells. We found that expression of *Dictyostelium* LMM leads to the complete loss of myosin II function. The cells containing LMM fail to undergo cytokinesis, fail to cap Con A receptors and fail to complete the *Dictyostelium* developmental

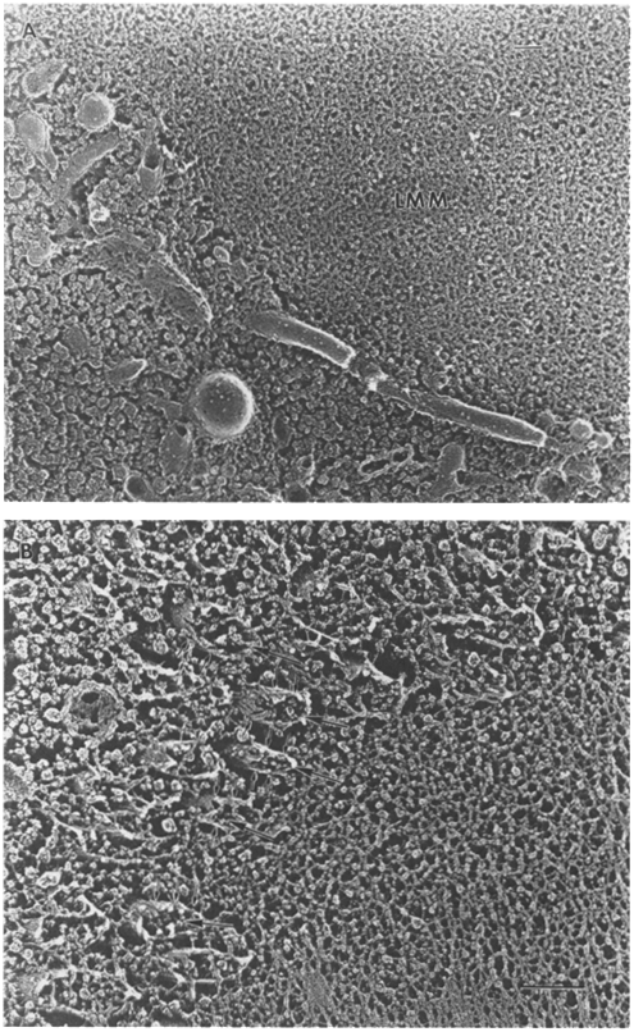

Figure 9. Deep-etch microscopy of the LMM structures. Deep-etch views of the LMM *Dictyostelium* mutants that were quick-frozen, without prior chemical fixation or cryoprotection, then fractured and deep-etched to reveal their cytoplasmic interiors. Portions of two large LMM aggregates are shown in the upper and lower right-hand portions of *A* and *B*, respectively. At lower magnification in panel *A*, the uniform density of the LMM aggregate is illustrated, highlighted by its exclusion of all surrounding cytoplasmic organelles. At higher magnification in *B*, the interior of the aggregate appears to be a dense meshwork of fine fibrils and globules (mostly representing fractured fibrils). Surrounding the aggregate and demarcating it from the rest of the cytoplasm are a number of tubular LMM structures with fibrils of about 15 nm. The walls of these structures are indicated by the small arrows and their lumens by the large arrows. Notice that these tubular structures are organized in a parallel array (cf. Fig. 8). Bars, 0.1 μm.

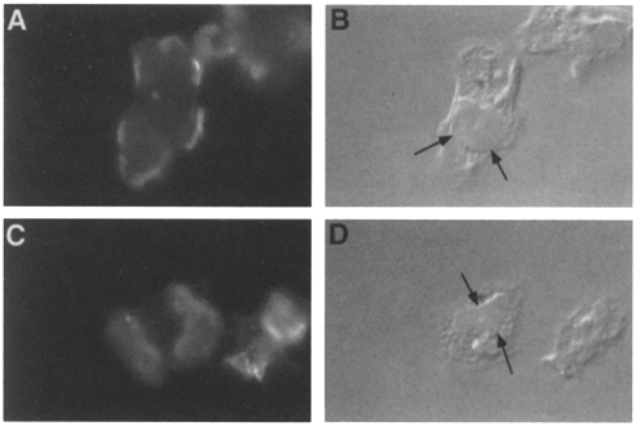

Figure 10. The large LMM aggregates do not contain F-actin. To determine if the large LMM aggregates found in the mutant cells were held together by F-actin we stained these cells with rhodamine–phalloidin (*A* and *C*). Actin was found prominently located in the cortex of the cell but it was never associated with the large clusters which are clearly seen by DIC microscopy (*B* and *D*, *arrows*). Most of the F-actin in these cells is out of the plane of focus where the LMM aggregates are found and, therefore, does not appear particularly bright in these images.

program. Therefore, expression of LMM acts as a dominant-negative mutation for myosin II function.

Since myosin II and LMM localize in the same structures in the mutant *Dictyostelium* amoebae, the most likely explanation for their myosin-null phenotype is that LMM sequesters most or all the native myosin molecules into these abnormal structures. Hence, myosin II would not be available to form the bipolar thick filaments required for its normal in vivo function. An alternate possibility considered at the outset of this study was that myosin II would still be able to form bipolar thick filaments in these cells, but the incorporation of LMM molecules into these filaments would disrupt their normal function. This idea was stimulated by our finding that the formation of single-headed myosin II in *Dictyostelium* cells leads to its incorporation into existent myosin filaments in a manner that disrupts myosin function in vivo (Burns et al., 1995). In contrast, the results described here illustrate that overexpression of LMM totally disrupts normal myosin filament formation by sequestering the native myosin II into abnormal aggregates.

Interestingly, the expressed LMM forms two different kinds of structures in vivo. We found arrays of long tubular structures and also large clusters of short and randomly oriented filaments. We do not know what factors determine these two configurations, but it is possible that they reflect different ratios in their content of myosin and LMM proteins. Our immunofluorescence studies indicate that both proteins are found in the two structures, however, we did not distinguish any differences in their relative distributions. Another possibility is that these two structures arise from interactions with different cellular components. The tubular structures, for example, are often found closely associated with the plasma membrane. This association may induce the extensive polymerization of the long tubular structures. Finally, an alternate possibility is that the two structures are formed by the presence or absence of different myosin binding proteins. The large cluster of filaments, for example, appears to be crosslinked by myriads of exceedingly fine filaments. However, the obvious candidate for such a crosslinker, namely F-actin, is not found in this aggregate. The fine filaments may be nothing more than individual LMM molecules that are shared between adjacent filaments and thus form a ran-

dom mesh. However, a more exciting possibility is that some other as yet uncharacterized myosin binding protein holds together the large clusters of filaments. Purification of the various myosin aggregates from these cells should help to distinguish among these possibilities.

The formation of these interesting structures is induced by the high levels of expression of LMM. We believe that these levels are a result of the stability of the LMM protein in vivo rather than due to the vector used. When we used the same vector to express the entire myosin II rod or the myosin S2 fragment we obtained much lower levels of expression (Burns et al., 1995). Furthermore, we were never able to alter the levels of expression of LMM nor did we isolate a transformant cell line that expressed different amounts of LMM. This suggests that when the LMM protein is expressed and assembles into the abnormal structures it becomes protected from degradation and accumulates to very high levels. Other myosin fragments that are soluble (S2 fragment) or that do not assemble into abnormal structures (myosin rod) are probably subject to the same turnover rate of the native myosin II and do not accumulate to high levels. This result suggests a novel method for the disruption of myosin II function without the ablation of the myosin II heavy or light chain genes in *Dictyostelium.* A gene knockout strategy does not allow for the study of myosin function in a particular cell type since all cells in the aggregate would be mutant. The only available method to disrupt myosin expression in a particular cell type is to produce an antisense mRNA with a cell-type specific promoter. This method, however, is very unreliable since high levels of antisense mRNA must be produced and do not always produce an effect. On the other hand, expression of LMM under the same cell-type specific promoter may cause the accumulation of high levels of LMM as shown here. LMM in those cells would then sequester the native myosin into abnormal structures and would obliterate myosin II function in that cell-type without affecting other cell types.

The dominant–negative effect of LMM expression also provides an excellent system to determine the specific sequences involved in filament formation. It should be straightforward to screen for mutations in the LMM sequence that impair its ability to self-associate. Such a mutation would produce an LMM molecule that is soluble and, as a result, that would not disturb myosin II function.

We thank Dr. Bruce Nicklas for his help and advice in the use of the polarized-light microscope, and Nancy Kaufmann for her help with immunofluorescence microscopy.

This research was supported by grants from the North Carolina Biotechnology Center and the Council for Tobacco Research to A. De Lozanne and from National Institutes of Health to M. K. Reedy and J. E. Heuser.

Received for publication 2 May 1995 and in revised form 8 May 1995.

References

Beinbrech, G., F. T. Ashton, and F. A. Pepe. 1988. Invertebrate myosin filament: subfilament arrangement in the wall of tubular filaments of insect flight muscles. *J. Mol. Biol.* 201:557–565.

Berlot, C. H., P. N. Devreotes, and J. A. Spudich. 1987. Chemoattractant-elicited increases in *Dictyostelium* myosin phosphorylation are due to changes in myosin localization and increases in kinase activity. *J. Biol. Chem.* 262:3918–3926.

Burns, C. G., D. A. Larochelle, H. Erickson, M. Reedy, and A. De Lozanne. 1995. Single-headed myosin II acts as a dominant-negative mutation in *Dictyostelium. Proc. Natl. Acad. Sci. USA.* In press.

De Lozanne, A. 1988. Myosin structure and function: molecular genetic studies of *Dictyostelium* myosin. Stanford University, Ph. D. Thesis. 189 pp.

De Lozanne, A., and J. A. Spudich. 1987. Disruption of the *Dictyostelium* myosin heavy chain gene by homologous recombination. *Science (Wash. DC).* 236:1086–1091.

De Lozanne, A., C. H. Berlot, L. A. Leinwand, and J. A. Spudich. 1987. Expression in *Escherichia coli* of a functional *Dictyostelium* myosin tail fragment. *J. Cell Biol.* 105:2999–3005.

Egelhoff, T. T., S. S. Brown, and J. A. Spudich. 1991. Spatial and temporal control of nonmuscle myosin localization identification of a domain that is necessary for myosin filament disassembly in vivo. *J. Cell Biol.* 112:677–688.

Fukui, Y., A. De Lozanne, and J. A. Spudich. 1990. Structure and function of the cytoskeleton of a *Dictyostelium* myosin-defective mutant. *J. Cell Biol.* 110:367–378.

Heuser, J. 1989. Effects of cytoplasmic acidification on clathrin lattice morphology. *J. Cell Biol.* 108:401–411.

Kubalek, E. W., T. Q. P. Uyeda, and J. A. Spudich. 1992. A *Dictyostelium* myosin II lacking a proximal 58-kDa portion of the tail is functional *in vitro* and *in vivo. Mol. Biol. Cell.* 3:1455–1462.

Lee, R. J., T. T. Egelhoff, and J. A. Spudich. 1994. Molecular genetic truncation analysis of filament assembly and phosphorylation domain of *Dictyostelium* myosin heavy chain. *J. Cell Sci.* 107:2875–2886.

Manstein, D. J., M. A. Titus, A. De Lozanne, and J. A. Spudich. 1989. Gene replacement in *Dictyostelium*: generation of myosin null mutants. *EMBO (Eur. Mol. Biol. Organ.) J.* 8:923–932.

McNally, E., R. Sohn, S. Frankel, and L. Leinwand. 1991. Expression of myosin and actin in *Escherichia coli. Methods Enzymol.* 196:368–389.

Nyitray, L., G. Mocz, L. Szilagyi, M. Balint, R. C. Lu, A. Wong, and J. Gergely. 1983. The proteolytic substructure of light meromyosin. *J. Biol. Chem.* 258: 13213–13220.

O'Halloran, T. J., and J. A. Spudich. 1990. Genetically engineered truncated myosin in *Dictyostelium*: the carboxyl-terminal regulatory domain is not required for the developmental cycle. *Proc. Natl. Acad. Sci. USA.* 87:8110–8114.

O'Halloran, T. J., S. Ravid, and J. A. Spudich. 1990. Expression of *Dictyostelium* myosin tail segments in *Escherichia coli*: domains required for assembly and phosphorylation. *J. Cell Biol.* 110:63–70.

Reedy, M. K., and M. C. Reedy. 1985. Rigor crossbridge structure in tilted single filament layers and flared-X formations from insect flight muscle. *J. Mol. Biol.* 185:145–176.

Spudich, J. A., editor. 1987. *Dictyostelium discoideum*: Molecular Approaches to Cell Biology. *In* Methods in Cell Biology. Academic Press, Inc., Orlando, Florida. 28:516 pp.

Vaillancourt, J. P., C. Lyons, and G. P. Côtè. 1988. Identification of two phosphorylated threonines in the tail region of *Dictyostelium* myosin II. *J. Biol. Chem.* 263:10082–10087.